iScience, Volume *24*

Supplemental information

Comparative analysis of clonal evolution among patients with right- and left-sided colon and rectal cancer

Santasree Banerjee, Xianxiang Zhang, Shan Kuang, Jigang Wang, Lei Li, Guangyi Fan, Yonglun Luo, Shuai Sun, Peng Han, Qingyao Wu, Shujian Yang, Xiaobin Ji, Yong Li, Li Deng, Xiaofen Tian, Zhiwei Wang, Yue Zhang, Kui Wu, Shida Zhu, Lars Bolund, Huanming Yang, Xun Xu, Junnian Liu, Yun Lu, and Xin Liu

Supplementary Figures

Figure S1

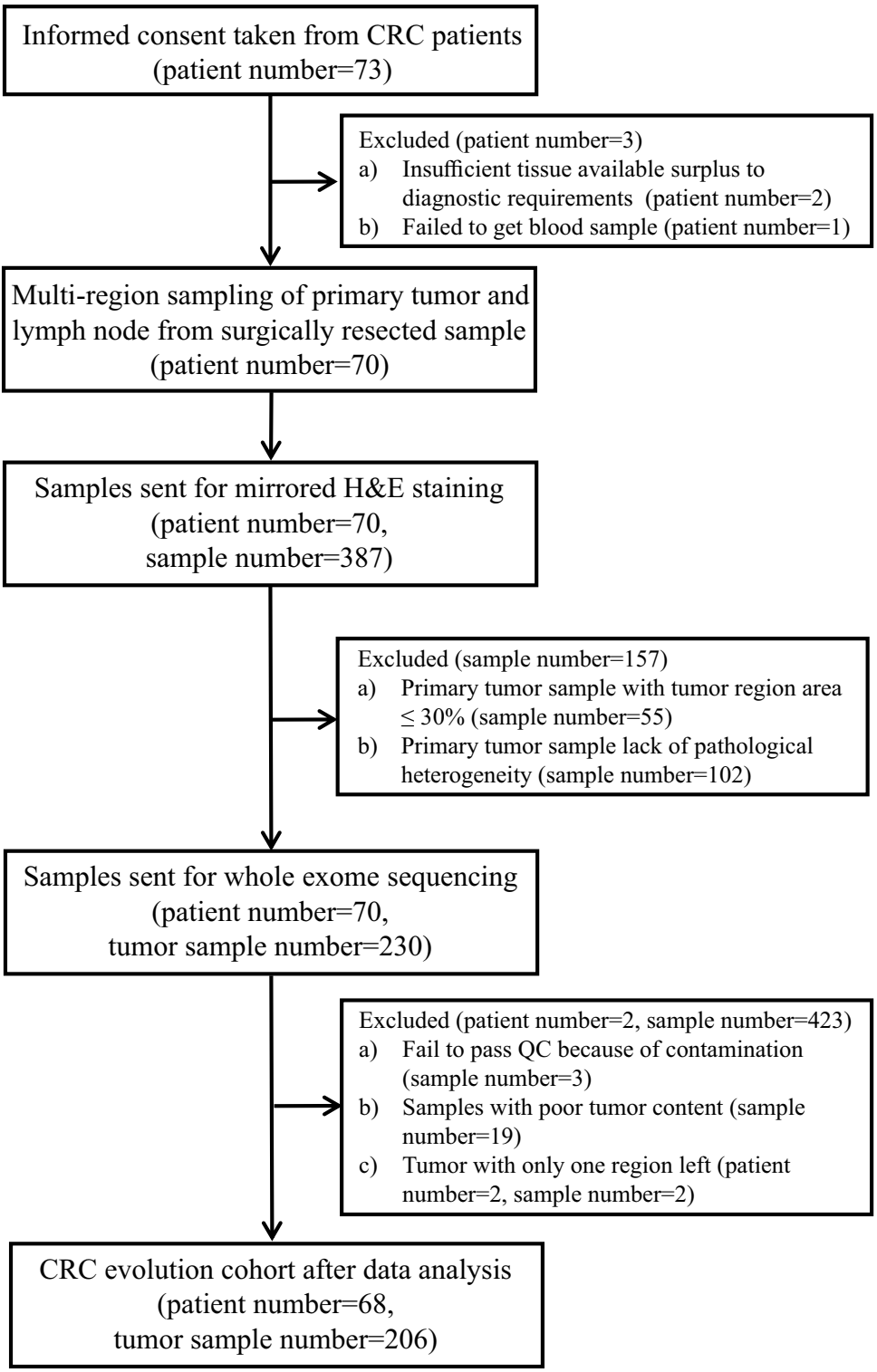

Figure S1. CONSORT diagram for patient recruitment in this study and eventual selection of the 68 patients cohort, Related to STAR Methods.

Figure S2

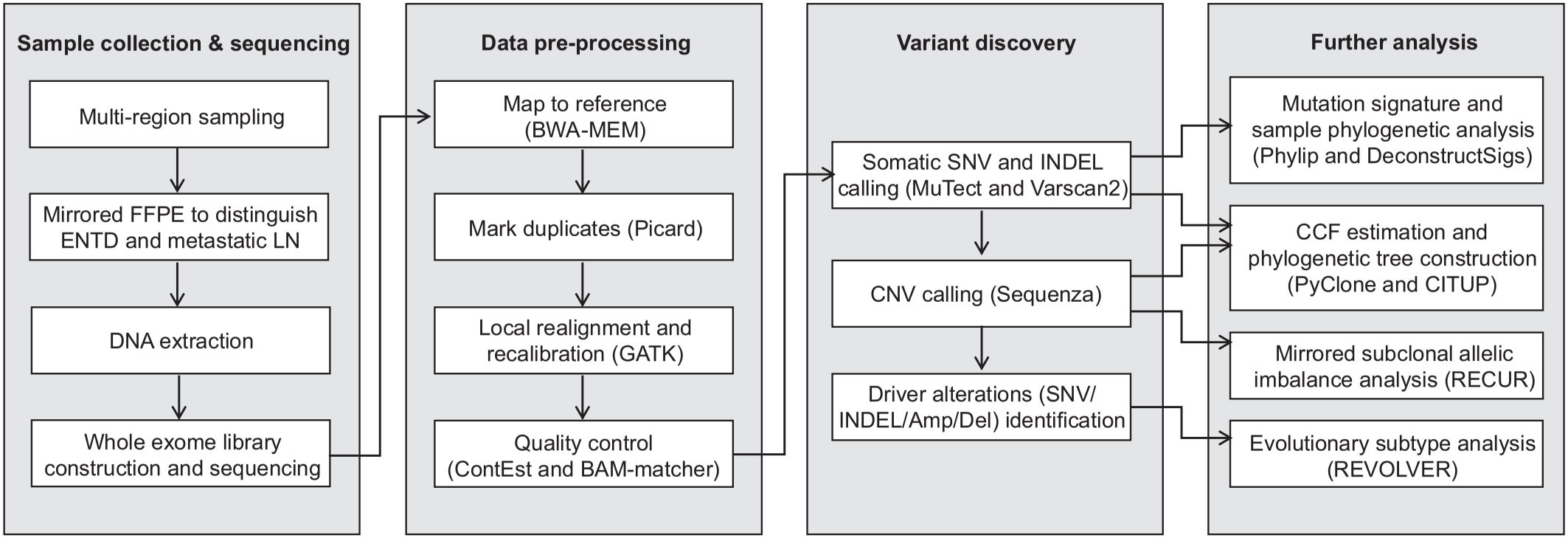

Figure S2. Workflow summarizing experiments and data analysis, Related to STAR Methods.
Overview of experiments and analysis workflow based on whole-exome sequencing of multi-region CRC tumors (primary tumors, lymph node metastasis and ENTDs) and paired normal controls. Analysis tools/methods are indicated by parentheses.

Figure S3

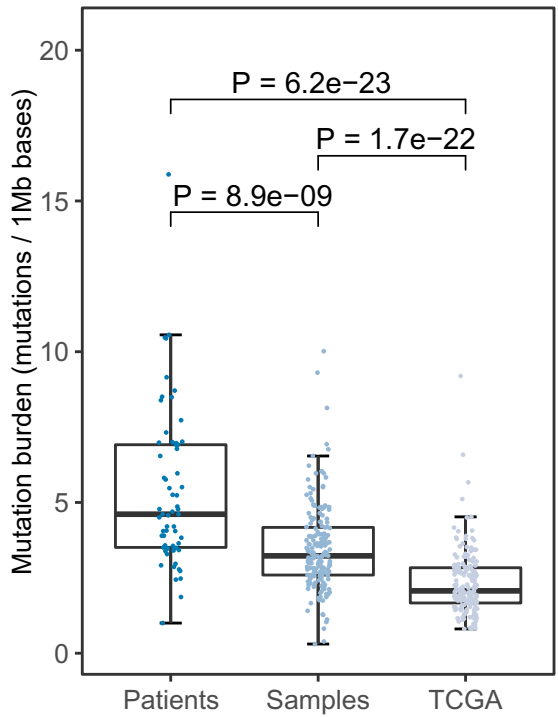

Figure S3. Comparison of tumor mutation burden between TCGA and CRC tumors, Related to Figure 1.

Box plots of mutation burden in non-hypermutated CRC patients analyzed as single samples, multi-region samples of non-hypermutated CRC patients and TCGA non-hypermutated CRC samples. The definition of hypermutated patients is all the samples in these patients have more than 10 mutations/1 Mb bases. In our CRC tumors, 6 patients are hypermutated patients and all other 62 patients are included into analysis.

Figure S4

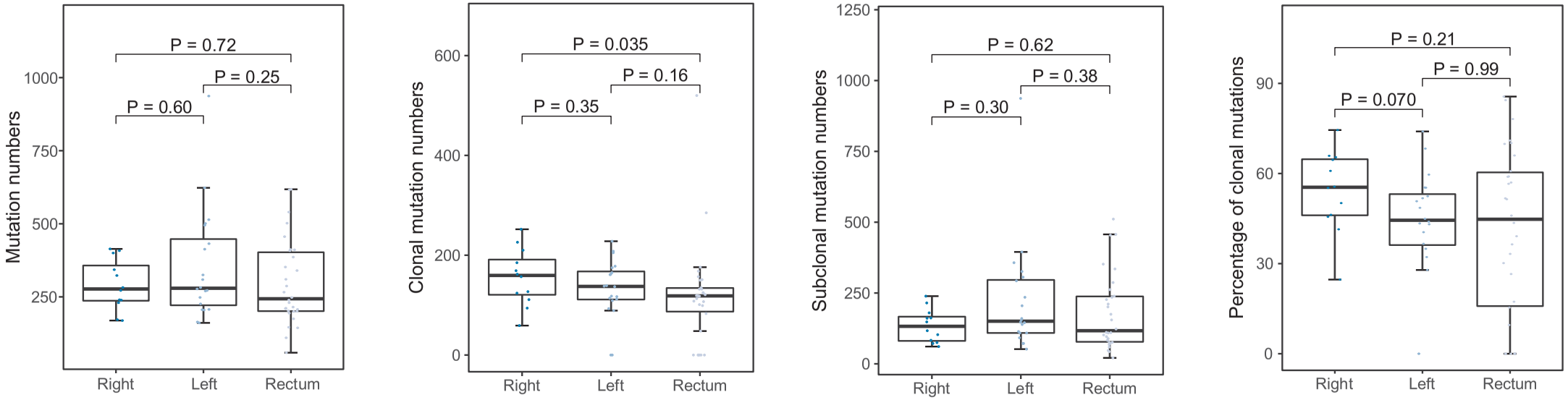

Figure S4. Intratumor heterogeneity of mutations among right-sided colon, left-sided colon and rectal cancers, Related to Figure 1. Box plots of total, clonal, subclonal and percentage of clonal mutations by tumor position.

Figure S5

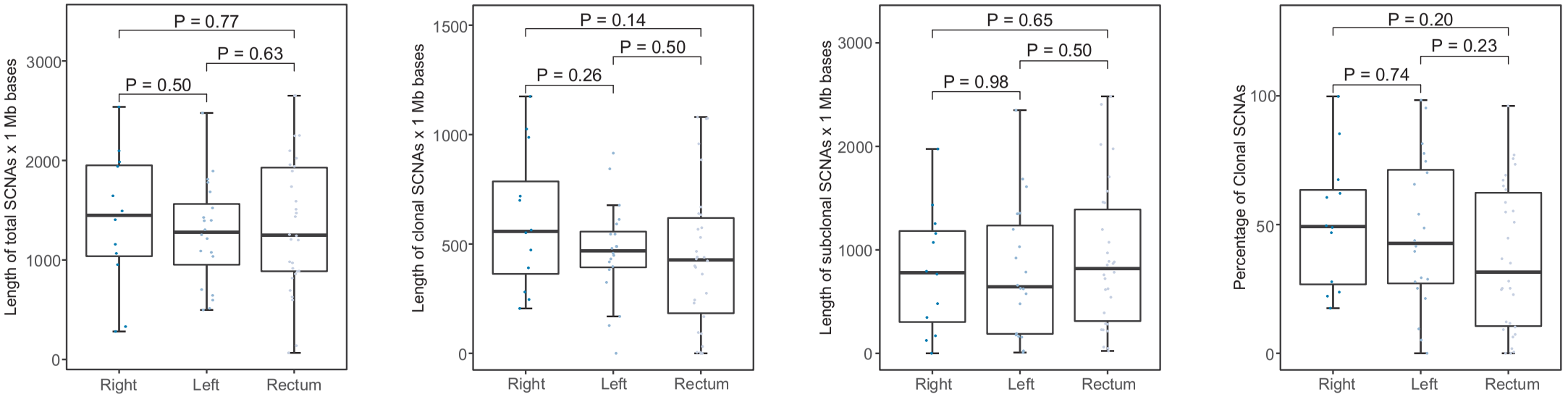

Figure S5. Intratumor heterogeneity of somatic copy number alterations (SCNAs) between right-sided colon, left-sided colon and rectal cancers, Related to Figure 1.

Box plots of total, clonal, subclonal and percentage of clonal SCNAs by tumor position.

Figure S6

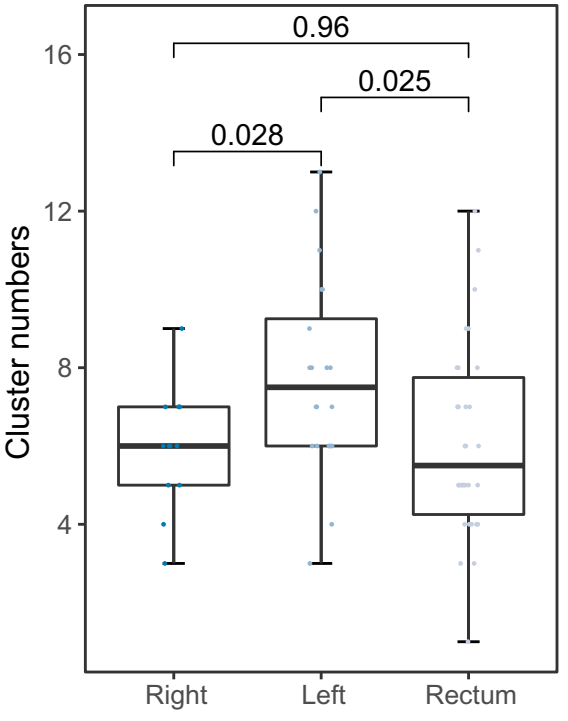

Figure S6. Difference of cluster numbers in CRC tumors between right-sided colon, left-sided colon and rectal cancers, Related to Figure 2.
Box plots of cluster numbers in CRC tumors by position.

Figure S7

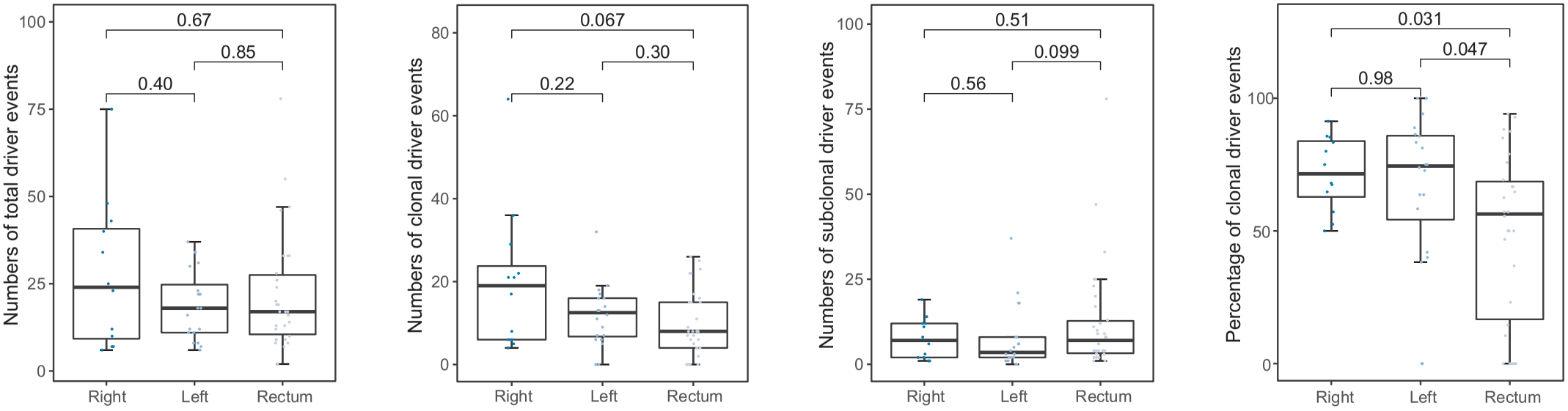

Figure S7. Difference in numbers of driver events in CRC tumors among right-sided colon, left-sided colon and rectal cancers, Related to Figure 3. Box plots of total, clonal, subclonal and percentage of clonal numbers of driver events by tumor position.

Figure S8

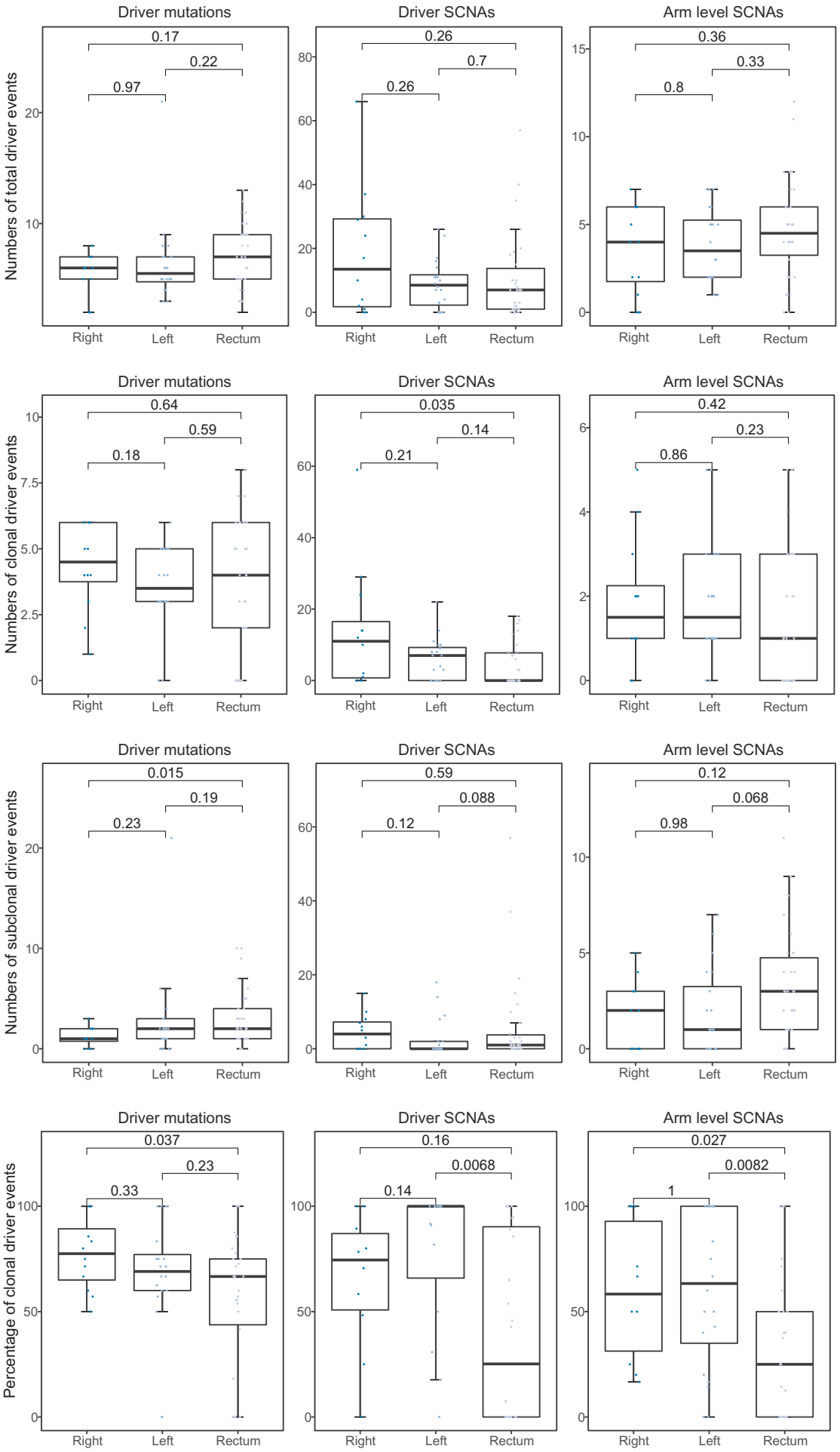

Figure S8. Difference in types of driver events in CRC tumors among right-sided colon, left-sided colon and rectal cancers, Related to Figure 3.

Box plots of total, clonal, subclonal and percentage of clonal numbers of different driver events types by tumor position.

Figure S9

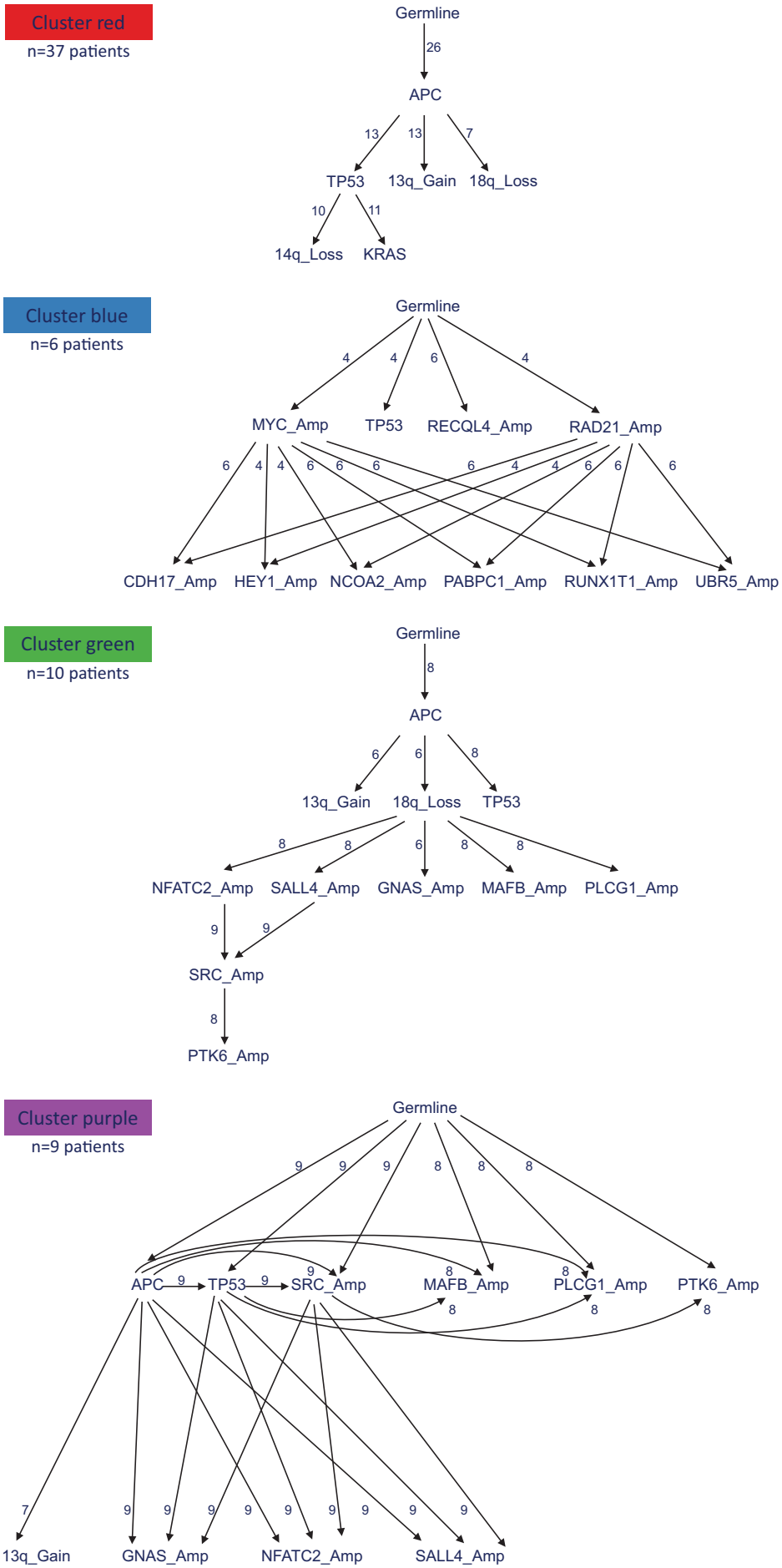

Figure S9. Repeated evolutionary trajectories, Related to Figure 4.
Repeated evolutionary trajectories of 4 clusters. The group size (n) and the number of times a trajectory was detected within the group on the edge were shown. Trajectories occurring ≥ 6 times in cluster red, green and purple were shown and trajectories occurring ≥ 4 times in cluster blue were shown.

Figure S10

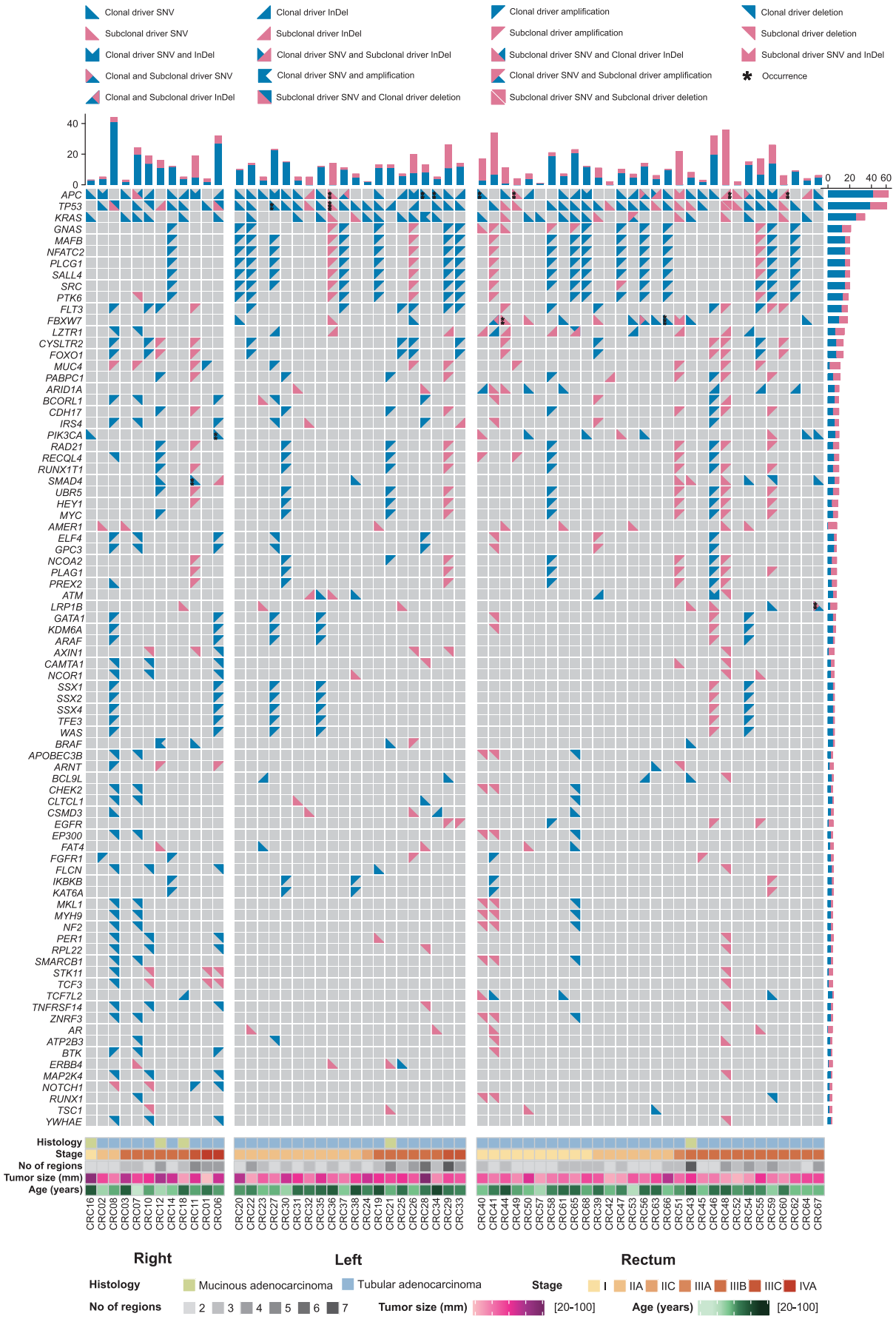

Figure S10. Heterogeneity of driver alterations in CRC tumors, Related to STAR Methods. Driver alterations detected in each tumor. Only genes containing ≥ 4 driver alterations across the CRC patients were included. The shape and color represented the alteration type and clonal status as shown in the top panel. The second top panel displayed the number of driver alterations identified across individual CRC tumors and the bar plots to the right showed the number of the variants in right-sided colon, left-sided colon and rectal cancers for each gene. The lower panel showed the demographic and clinical characteristics of the 62 CRC patients in this study (divided by histology; stage; number of regions; tumor size; age and tumor position).

Figure S11

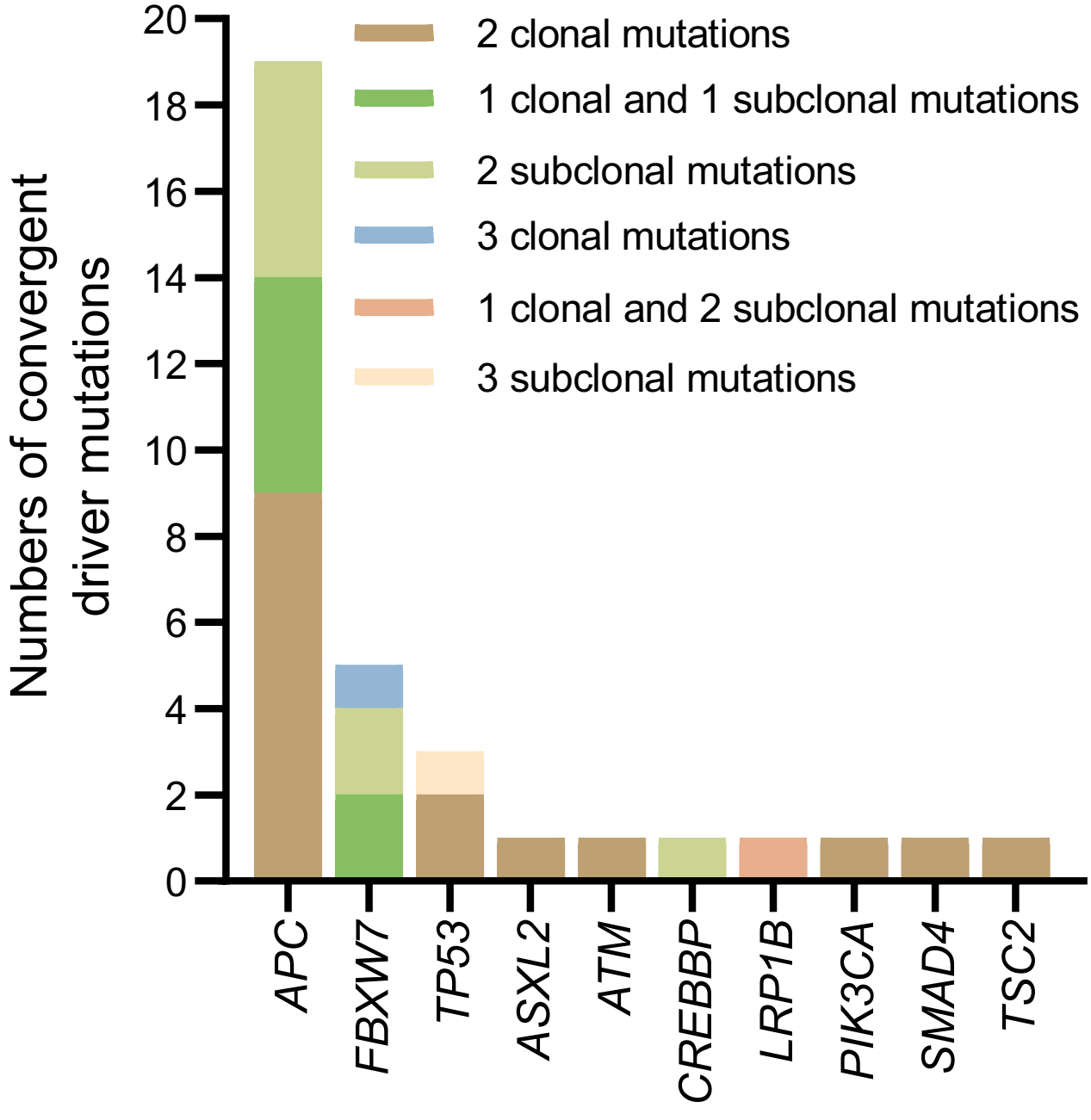

Figure S11. Convergent driver mutations in CRC tumors, Related to STAR Methods.

All convergent driver mutation events were summarized in 62 CRC tumors.

Figure S12

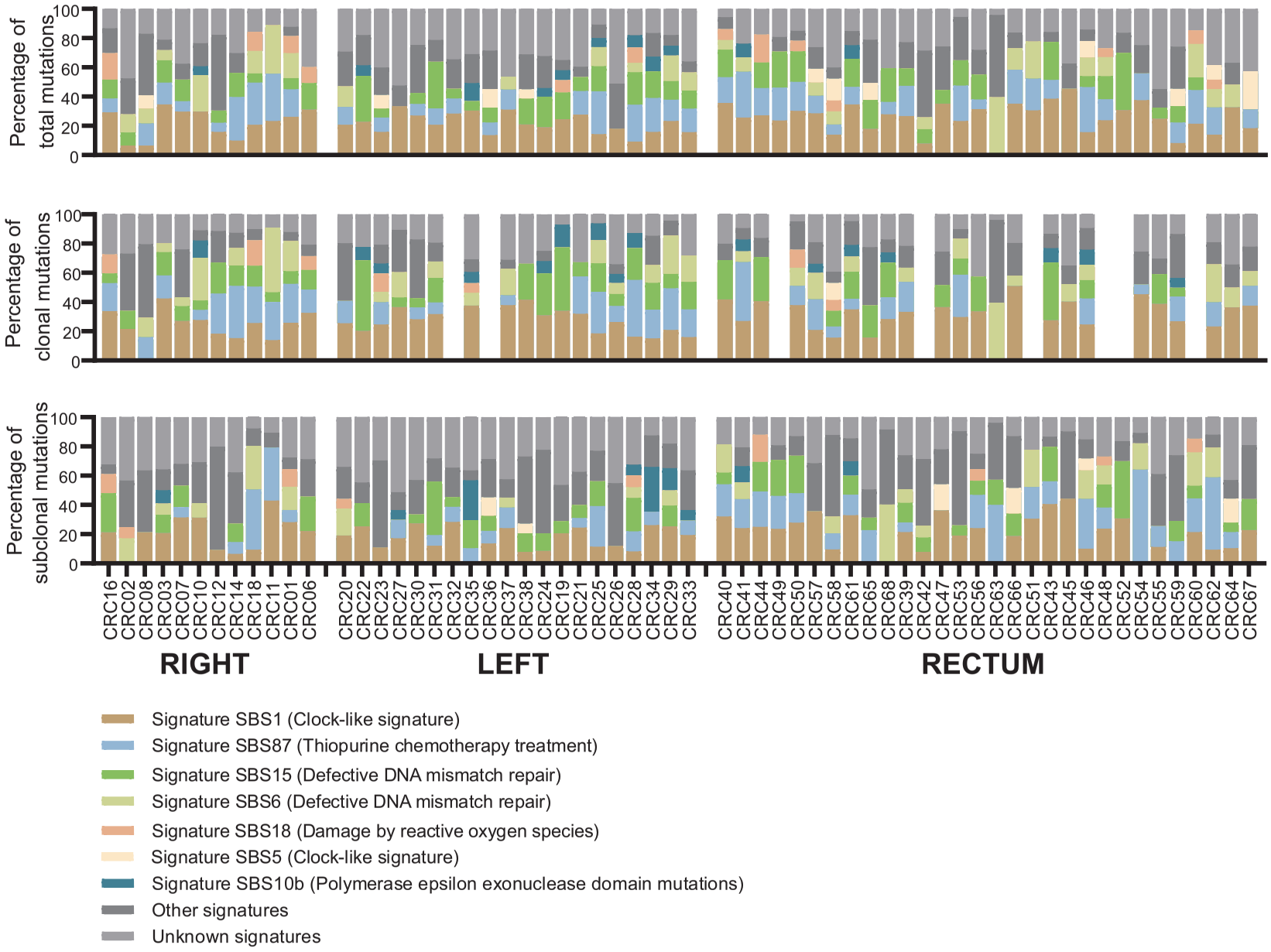

Figure S12. Mutation signature in CRC tumors, Related to STAR Methods.
Mutation signatures identified in CRC tumors, split according to tumor position and clonality of mutations.

Figure S13

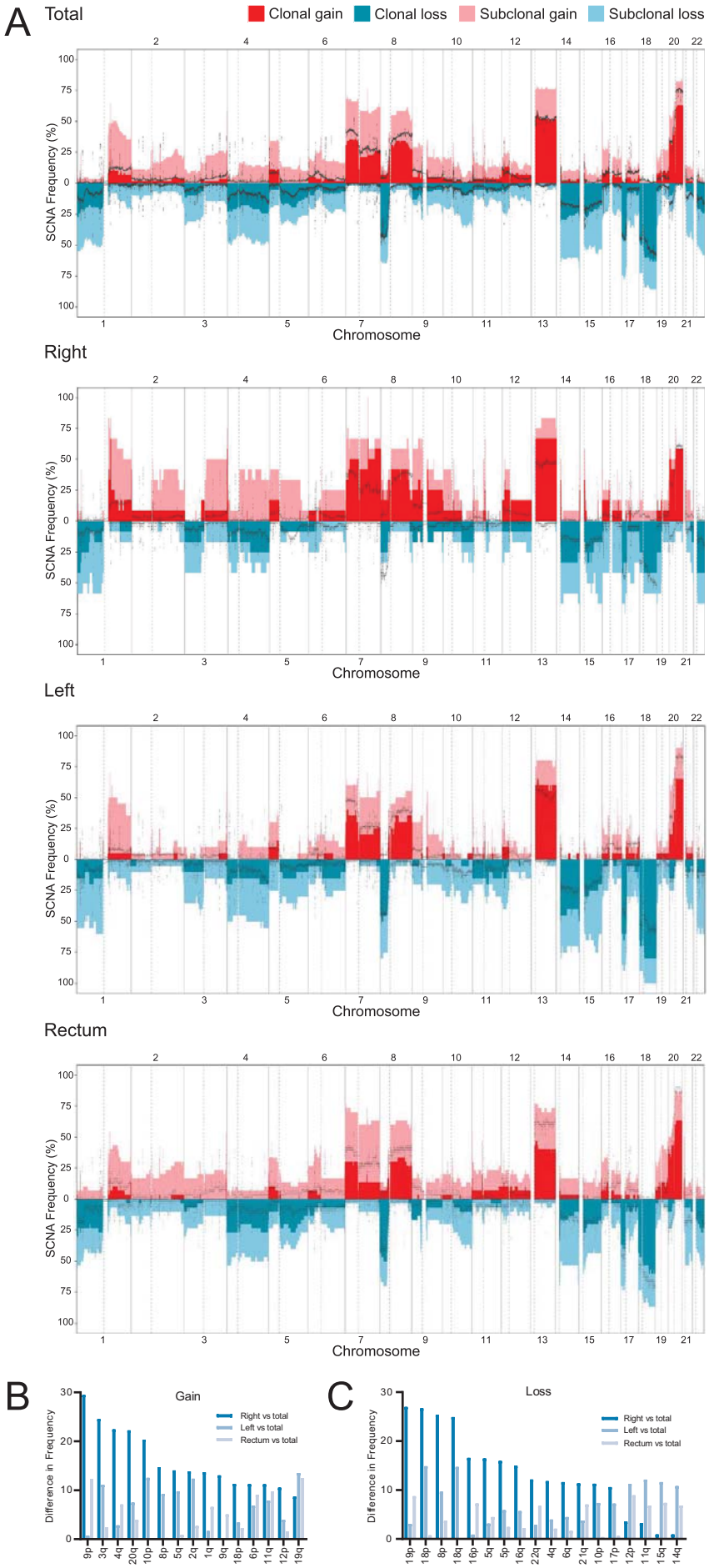

Figure S13. Differences in SCNA frequencies among total, right-sided colon, left-sided colon and rectal cancers, Related to STAR Methods.

(A) SCNA frequency of CRC tumors based on position. The black dots were frequency of SCNAs among total, right-sided colon, left-sided colon and rectal cancers in TCGA CRC samples.

(B) and (C) The mean frequency of each chromosome arm by tumor position were calculated and only the chromosome arm with absolute difference of more than 10% were shown.

Figure S14

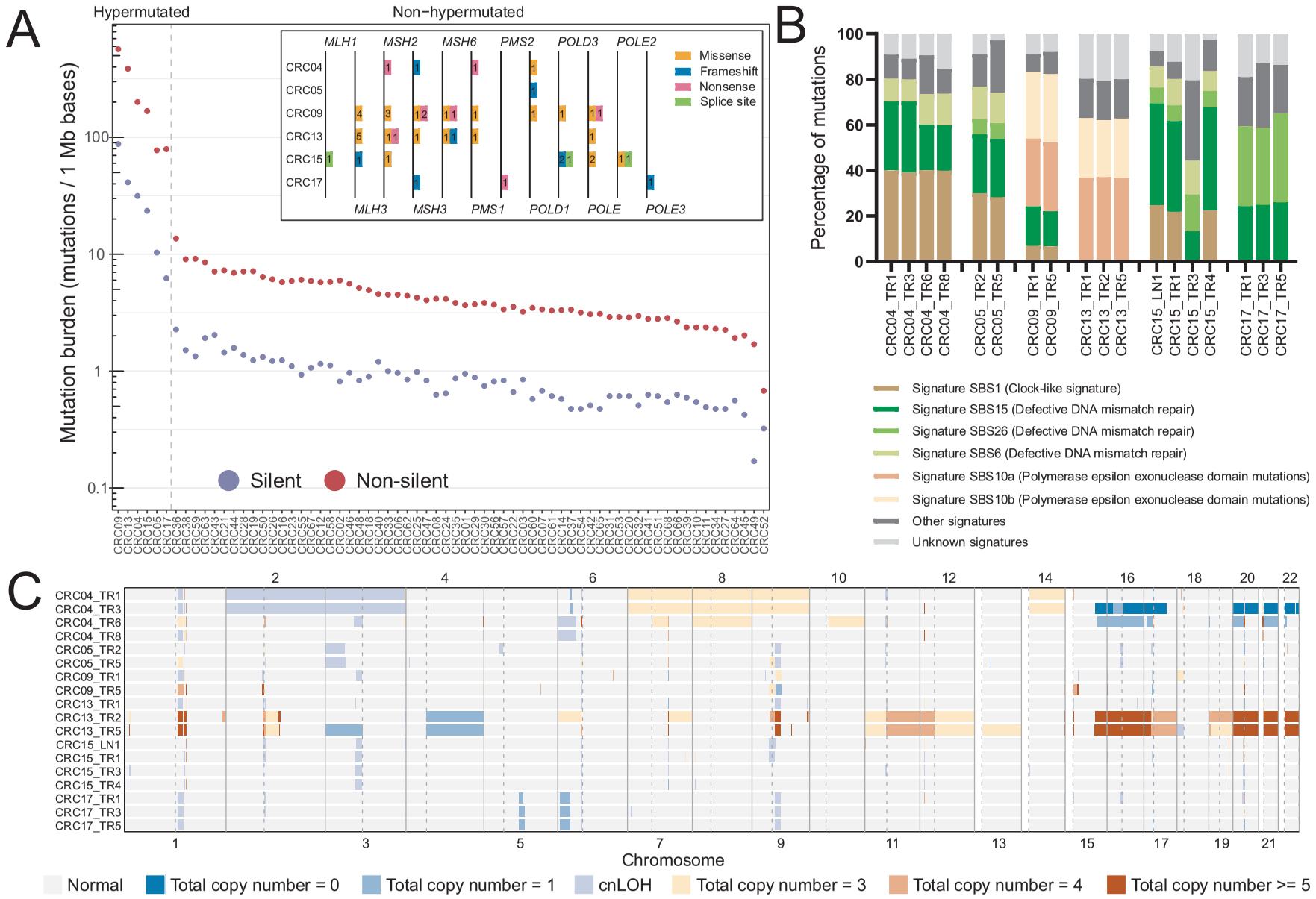

Figure S14. Intratumor heterogeneity landscape of hypermutated CRC tumors, Related to STAR Methods.

(A)Mutation burden of 68 CRC tumors. Inset, mutations in mismatch-repair genes, *POLE* and *POLD* gene family among the hypermutated tumors. The definition of hypermutated tumors was that all the sample in that tumor had more than 10 mutations/1 Mb bases.

(B)Mutation signature of all the samples from 6 hypermutated CRC tumors.

(C)Heatmap of genome-wide view SCNAs in 6 hypermutated CRC tumors.

Figure S15

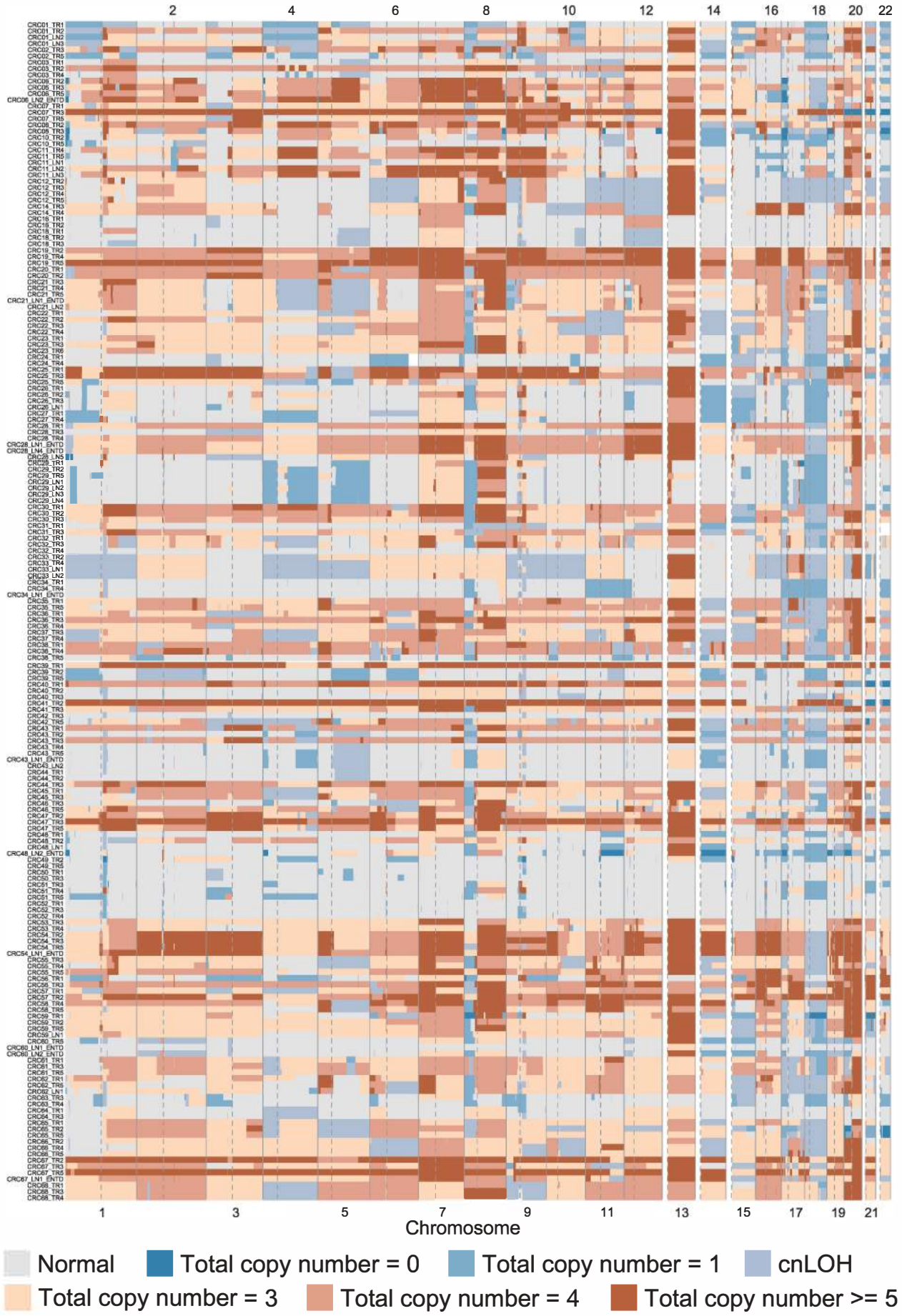

Figure S15. Heatmap of SCNAs among non-hypermutated CRC tumors, Related to STAR methods.

Heatmap of genome-wide view SCNAs were shown for all the regions of non-hypermutated CRC tumors by position.

Figure S16

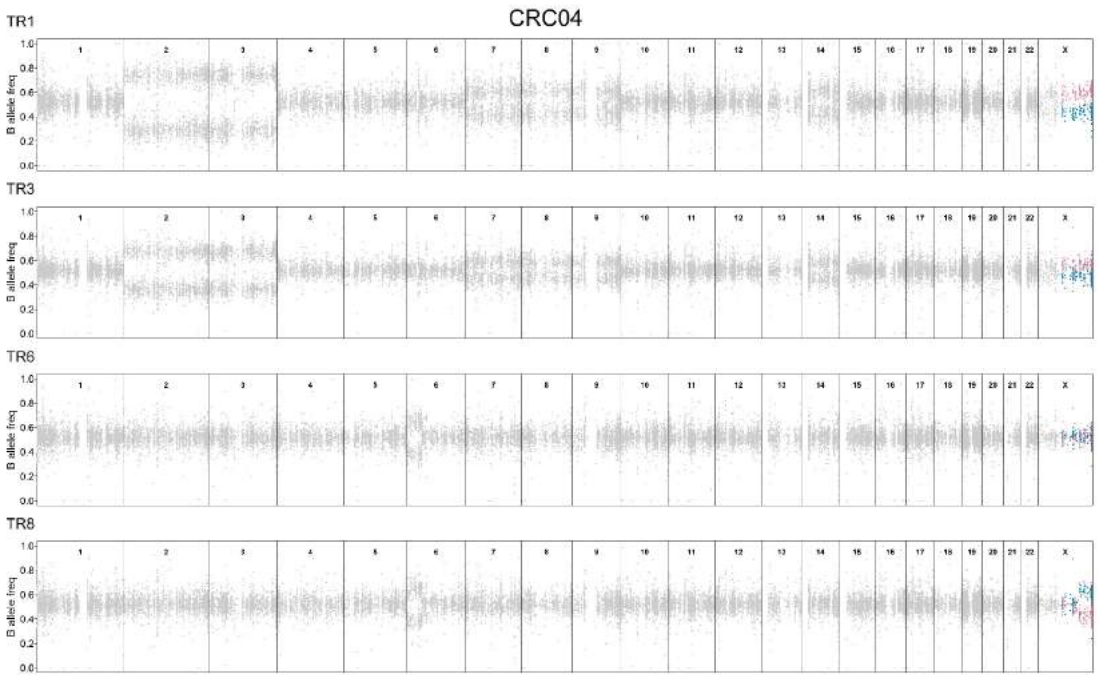

Figure S16. MSAI events in hypermutated CRC tumor, Related to Figure 6.
B-allele frequency (BAF) profile of heterozygous SNPs across the genome (chromosomes 1-22, X) from all the regions of CRC04. Sections of BAF in regions that had MSAI were highlighted in blue or red.

Figure S17

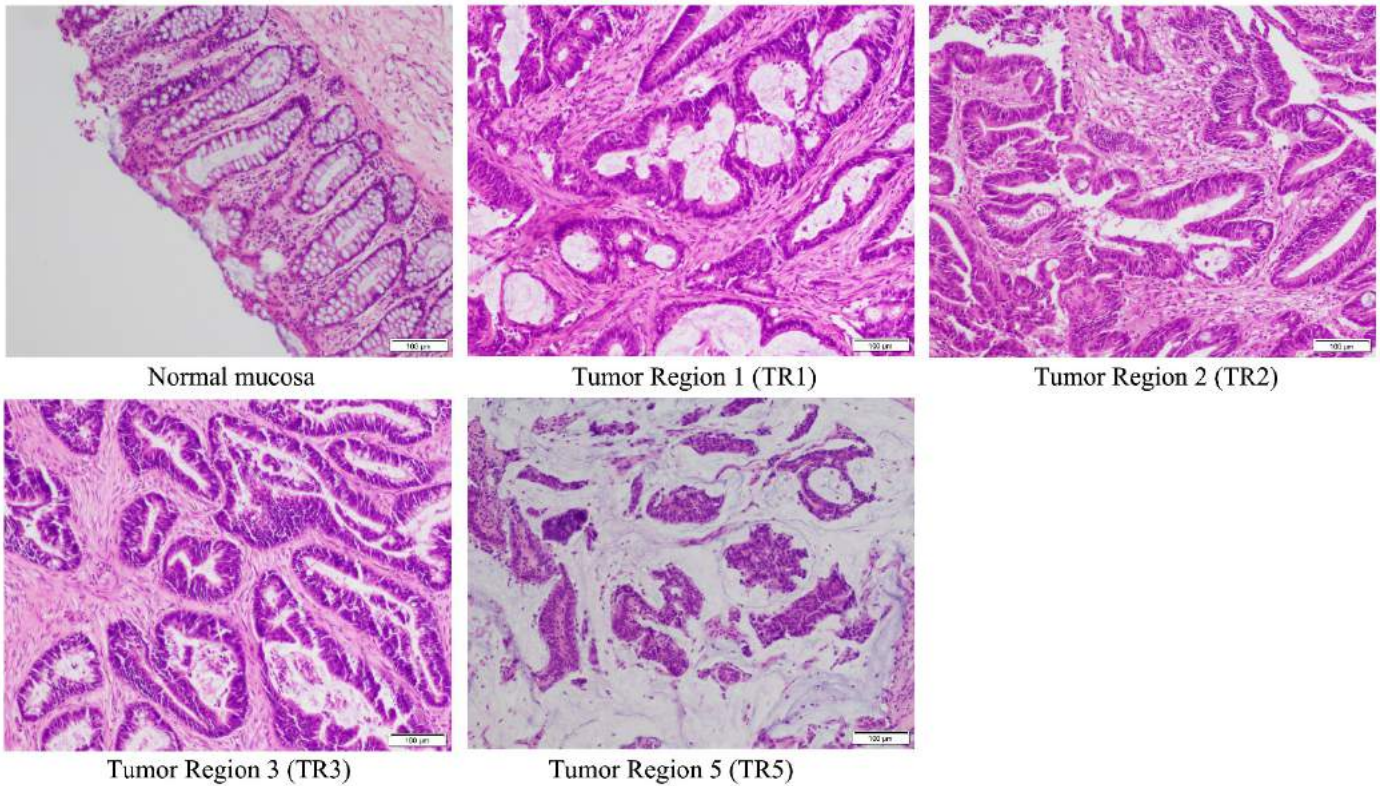

Figure S17. Hematoxylin and eosin staining of mirrored FFPE samples in CRC09, Related to STAR methods.

Photomicrographs of Hematoxylin and eosin stains of normal mucosa and multiregional tumor samples collected from CRC09 patient. Tumor region 4 was deleted because of less than 30% tumor component. Scale bars indicate 100 μm.